

Supplementary information

for: Increasing organic solar cell efficiency with polymer interlayers.

Felix Deschler^a, Daniel Riedel^a, Bernhard Ecker^b, Elizabeth von Hauff^{bc},
Enrico Da Como^{ad}, and Roderick C I MacKenzie^{ef*}

a)Department of Physics and CeNS,
Ludwig-Maximilians-Universität München,
Amalienstr. 54, D-80799 München, Germany

b)Institute of Physics, Hermann-Herder-Str. 3a,
D-79104, Freiburg, Germany

c)Fraunhofer Institute for Solar Energy Systems (ISE),
Heidenhofstr. 2, D-79110 Freiburg, Germany

d)Department of Physics, University of Bath,
Somerset, BA2 7AY (UK)

e)FRIAS, School of Soft Matter Research,
University of Freiburg, Albertstraße 19
79104 Freiburg, Germany

f)Faculty of Engineering, University of Nottingham,
Nottingham, Nottinghamshire, NG7 2RD (UK)

*e-mail: roderick.mackenzie@nottingham.ac.uk

November 4, 2012

1 Supplementary information

1.1 Device fabrication

The devices were fabricated on ITO/glass substrates, cleaned in an ultrasonic bath and subsequently in deionized water, acetone and isopropyl alcohol. The preparation of the polymer:PCBM blends was done in a nitrogen filled glovebox, in order to prevent degradation of the materials. The three polymer:fullerene systems were blended in the following ratios: poly(3-hexylthiophene):phenyl-C61-butyric acid methyl ester (P3HT:PCBM) blended 1:0.8 in chlorobenzene with an overall concentration of 54 *mg/ml*; poly[(4,4'-bis(2-ethylhexyl)dithiene[3,2-b:2',3'-d]silole)-2,6-diyl-alt-(4,7-bis(2-thienyl)-2,1,3-benzothiadiazole)-5,5'-diyl] (Si-PCPDTBT:PCBM) blended 1:2 in dichlorobenzene with an overall concentration of 30 *mg/ml*; and Poly[[4,8-bis[(2-ethylhexyl)oxy]benzo[1,2-b:4,5-b']dithiophene-2,6-diyl][3-fluoro-2-[(2-ethylhexyl)carbonyl]thieno[3,4-b]thiophenediyl]] (PTB7:PCBM) blended 1:1.5 in dichlorobenzene with an overall concentration of 25 *mg/ml*. For the bi-layer structures neat polymer solutions were prepared with an concentration of 2mg/ml in the respective solvent. The solutions were stirred at 70°C for around 20 hours prior application. For the preparation of solar cells, a 40 *nm* thin layer of PEDOT:PSS (Clevios P VP AI 4083) was spin coated on the ITO substrates in ambient atmosphere, annealed at 150°C for ten minutes and then brought into the glovebox, where all further processing steps were carried out. Mono-layer structures comprising a single bulk-heterojunction on top of the PEDOT:PSS and bi-layer structures including a neat polymer layer sandwiched between PEDOT:PSS and the bulk-heterojunction are prepared via spin coating. For the bi-layer structures the neat polymer films are annealed at 150°C for 20 minutes, prior application of the bulk-heterojunction layer to minimize the redissolution of the neat polymer layer. Finally a cathode consisting of 0.7 *nm* LiF and 100 *nm* Al were evaporated on top of the active layer under high vacuum. Thus solar cells with the following structures are obtained: glass/ITO/PEDOT:PSS/polymer:PCBM/LiF/Al and glass/ITO/PEDOT:PSS/polymer/polymer:PCBM/LiF/Al denoted as mono-layer and bi-layer respectively. A schematic of the bi-layer structure is shown in figure 1. Solar cells comprising P3HT were additionally annealed at 140°C for 20 minutes after device completion.

1.2 Model calibration

The fit of the model to the JV curves is shown in figure S1 and the model parameters are shown in table S1.

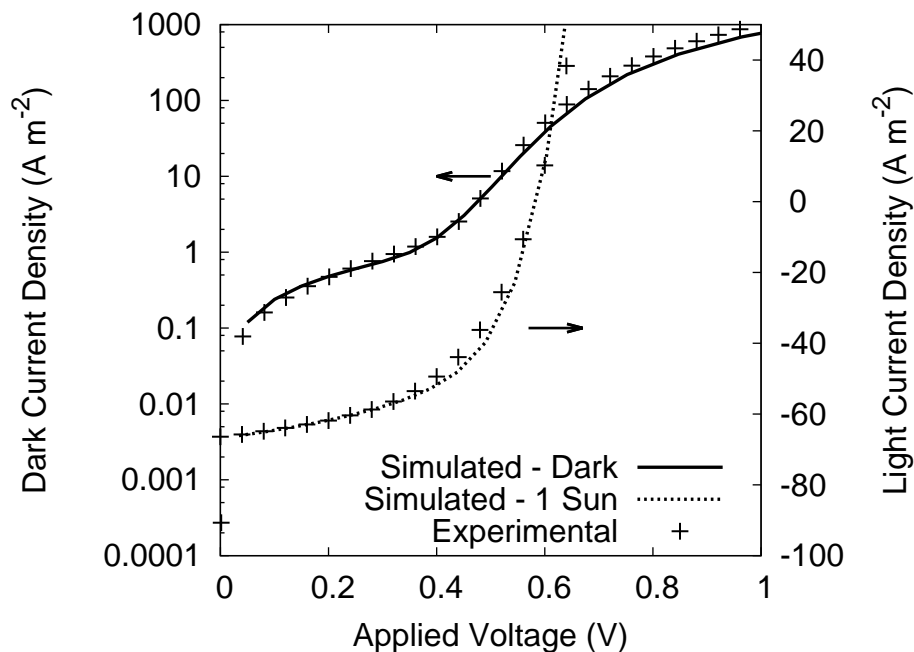


Figure S1: A fit of the model to the experimental light/dark JV curves for a representative P3HT:PCBM device.

Description	Parameter	Value
Left contact electron density	n_l	$1.88 \times 10^{26} m^{-3}$
Right contact hole density	p_r	$1.22 \times 10^{25} m^{-3}$
Effective electron trap density	N_e^{exp}	$1.0 \times 10^{26} m^{-3} eV^{-1}$
Effective hole trap density	N_h^{exp}	$4.8 \times 10^{24} m^{-3} eV^{-1}$
Characteristic energy for electron exponential tail	E_e^u	40 meV
Characteristic energy for hole exponential tail	E_h^u	90 meV
Effective density of free electron states	N_c	$2.83 \times 10^{26} m^{-3}$
Effective density of free hole states	N_v	$3.44 \times 10^{26} m^{-3}$
LUMO electron capture cross section	σ_e^e	$4.70 \times 10^{-21} m^{-2}$
LUMO hole capture cross section	σ_h^e	$2.81 \times 10^{-24} m^{-2}$
HOMO electron capture cross section	σ_e^h	$2.88 \times 10^{-23} m^{-2}$
HOMO hole capture cross section	σ_h^h	$6.87 \times 10^{-22} m^{-2}$
Free electron mobility	μ_{e0}	$4.40 \times 10^{-08} m^2 V^{-1} s^{-1}$
Free hole mobility	μ_{h0}	$6.70 \times 10^{-05} m^2 V^{-1} s^{-1}$

Table S1: The table of electrical model parameters

The exact form of the density of states in organic devices is a hotly debated topic within the literature

(10.1103/PhysRevB.86.115302, 10.1002/aenm.201100709). However, there is now significant evidence to suggest that the DoS is of exponential form. We therefore chose the LUMO and HOMO DoS to be exponential functions of form, $g(E) = N \exp(-E/E_{slope})$, where N is the magnitude of the DoS at the band edge and E_{slope} is the characteristic energy. (see 10.1002/aenm.201100709 for further information) The exact slope and magnitude of these DoS functions were allowed to vary (with the other model parameters) until they reproduced the experimental dark and light JV curves. It was the aim of the calibration procedure produce reasonable device parameters inline with previously reported data. It should be noted that without transient photocurrent data and charge extraction data (10.1002/aenm.201100709) the fitting procedure can only provide a reasonable set of device parameters not a unique set. More information about the model can be found at www.opvdm.com.

1.3 Optical Simulation

When simulating the propagation of light normally incident upon the surface of a solar cell it is common to use the transfer matrix method. In this method two equations are written for each optical mesh point within the device (J. Appl. Phys. 102, 054516 2007). One equation describes the forward traveling field and one the backwards traveling field. These two equations form a 2x2 matrix which describe reflection of light at dielectric interfaces, the loss due to absorption and change of phase of the field due to propagation within a single layer. To evaluate the electric field at any given mesh point one must perform a minimum of N 2x2 matrix multiplications. For each multiplication there is a computational overhead. This is not significant if the field is only calculated a few times or there are only a few mesh points. However for transient simulations or for fitting the model to experimental data this overhead can become significant. Therefore in this work rather than applying the traditional transfer matrix method directly we formed one large matrix of size 2Mx2M where M is the number of optical mesh points in the device. The top M diagonal matrix elements contained the terms describing the forward propagating field and the bottom M diagonal contained the equation representing the backwards propagating field. Off diagonal elements were introduced to take account of reflections. The forward and backwards propagating field were linked at the mesh point furthest away from the source assuming the incident wave was perfectly reflected on the metallic contact. In summary this method is mathematically identical to the transfer matrix method, the problem is just solved in one matrix by projecting it on to a finite difference mesh. We used the UMFPACK complex sparse solver to solve the set of linear equations.

1.4 EQE Spectra

In figure S2 the measured EQE spectra for the mono and bi-layers have been plotted. It can be seen that the EQE spectra for the bi-layer show higher efficiencies inline with what would be expected for a device with more photo-absorption and less recombination.

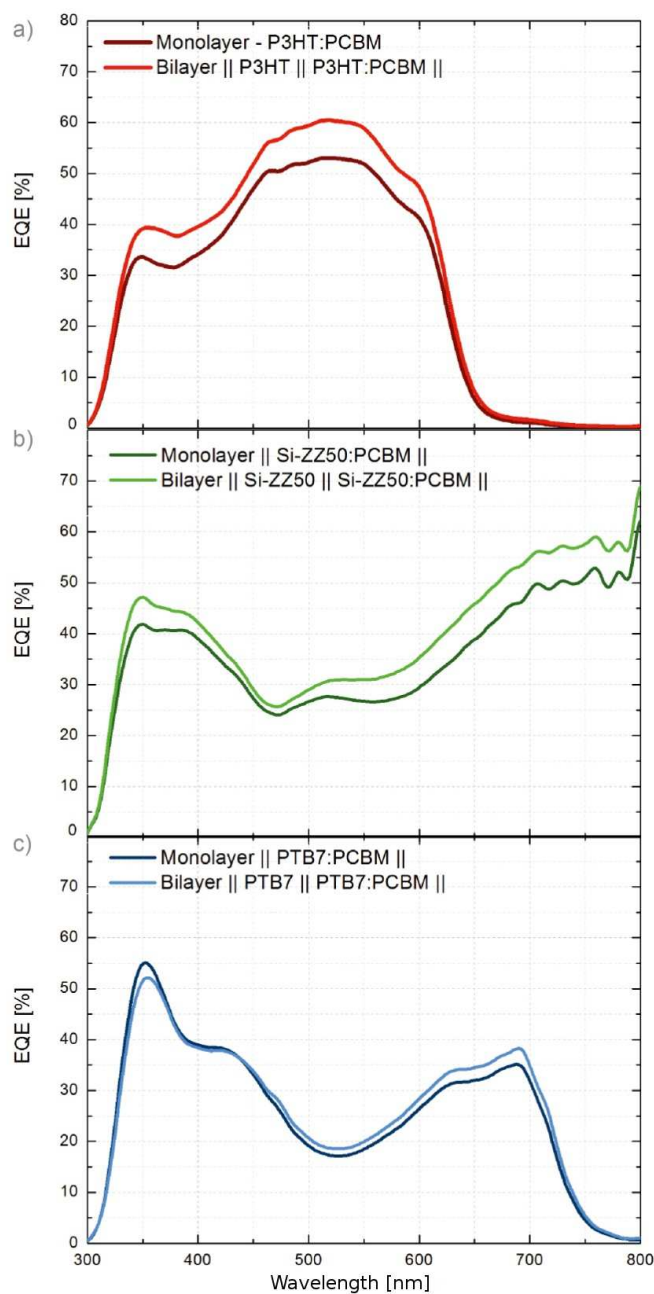


Figure S2: Improvement of EQE with the addition of the polymer layer. This supports the theory that the increase in efficiency is due to increased absorption and reduced recombination.

1.5 Testing the durability of the pure layer

To ensure that the pure polymer layer was not removed when a non-orthogonal solvent was used in the manufacture of the BHJ layer, we hardened the pure polymer layer by annealing at 150°C for 20 minutes. Then to test the durability of the hardened polymer layer we spin-coated the pure polymer layer with the same solvent used as used in the BHJ layer. It was found that for all layers the spin coating of the pure solvent reduced the layer thickness but crucially the layer was still present. An example of this is shown in figure S3.

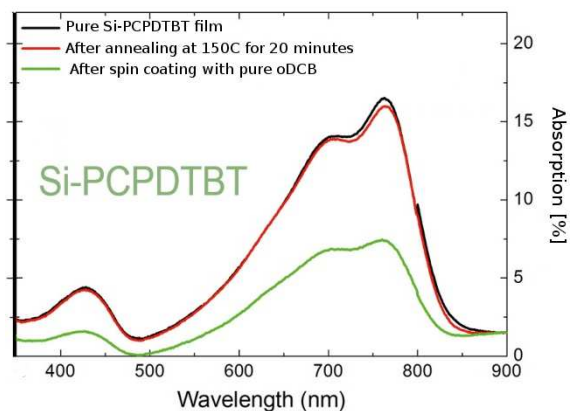


Figure S3: The UV-Vis spectra of a pure Si-PCPDTBT. Black line: film after deposition by spin coating. Red line: Spectra after annealing at 150°C for 20 minutes. Green line: Spectra after spin coating the annealed film with pure oDCB. It can be seen that although some of the film is removed by the oDCB the layer is still present.